



Paleoceanography and Paleoclimatology

Supporting Information for

A brGDGT-based reconstruction of terrestrial temperature from the Maritime Continent spanning the Last Glacial Maximum

M. C. Parish¹, X. Du^{1,2}, S. Bijaksana³, and J. M. Russell¹

¹Department of Earth, Environmental, & Planetary Sciences, Brown University, Providence, RI, USA.

² Institute at Brown for Environment and Society, Brown University, Providence, RI, USA

³ Global Geophysics Group, Faculty of Mining and Petroleum Engineering, Institut Teknologi Bandung, Bandung, Indonesia.

Contents of this file

Figures S1 to S3

Introduction

The supporting information includes Figure S1 and S2, which show all temperature reconstructions and GDGT-indices used to calculate Pearson's R in Figure 5. The supporting information also includes two pH reconstructions based on the fractional abundances of brGDGTs in the Lake Towuti record.

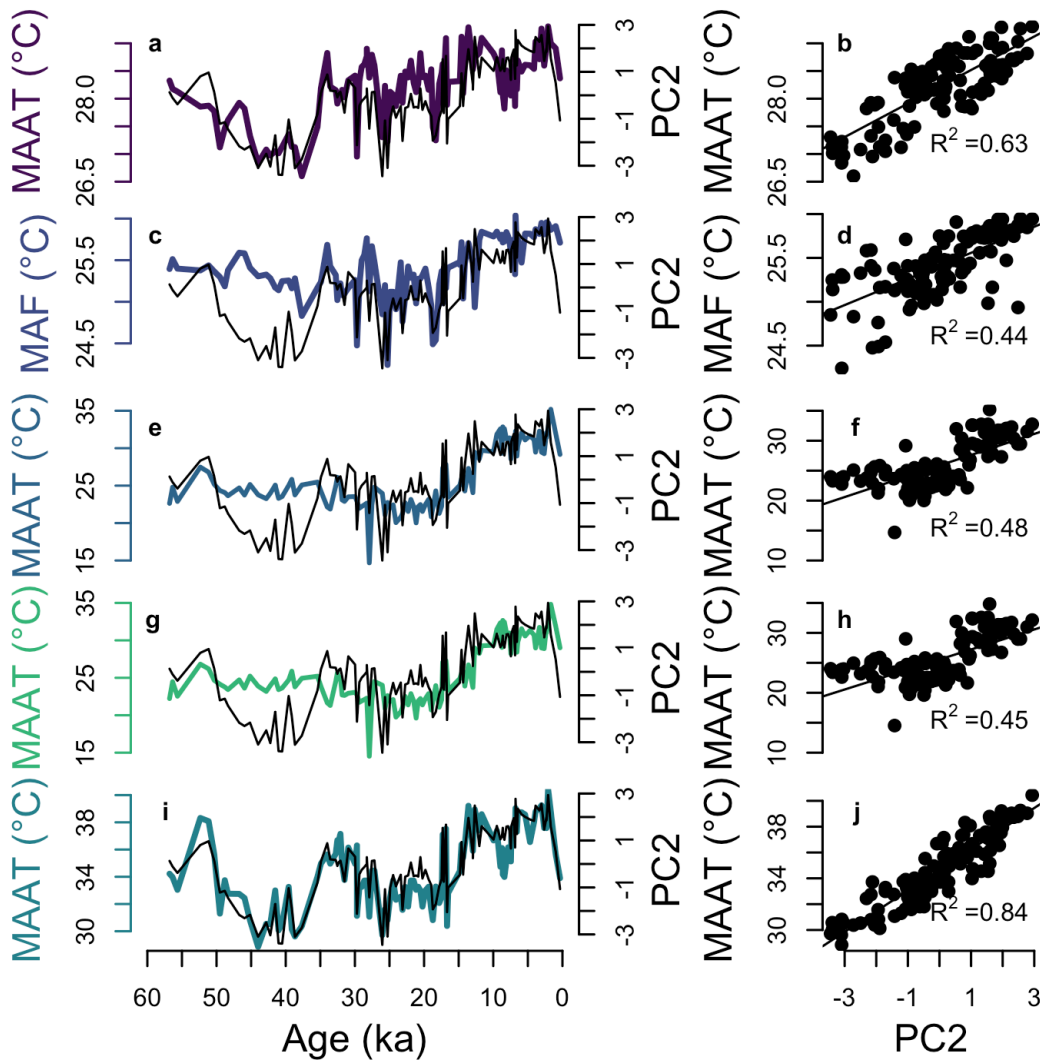


Figure S1. In Panels a, c, e, g, and i, the thin black line is PC2 from the principal component analysis, which we argue reflects temperature (see main text). Panels b, d, f, h, and j show regressions between PC2 and temperatures inferred from the different calibrations shown in panels a, c, e, g, and i, respectively. (a) Mean annual air temperature (MAAT) based on the MBT_{5ME} calibration from Russell et al. (2018) (purple). (c) Mean temperature of the months above freezing (MAF) calculated using the calibration from Raberg et al. (2021) for use in samples with small abundances of IIIb (purple). (e) SFS/SBE MAAT based on all global lacustrine samples from Martinez-Sosa et al. (2021). (g) SFS/SBE MAAT based only on surface samples with less than 50% hexmethylated brGDGTs. (i) SFS/SBE MAAT based on all samples from Russell et al. (2018).

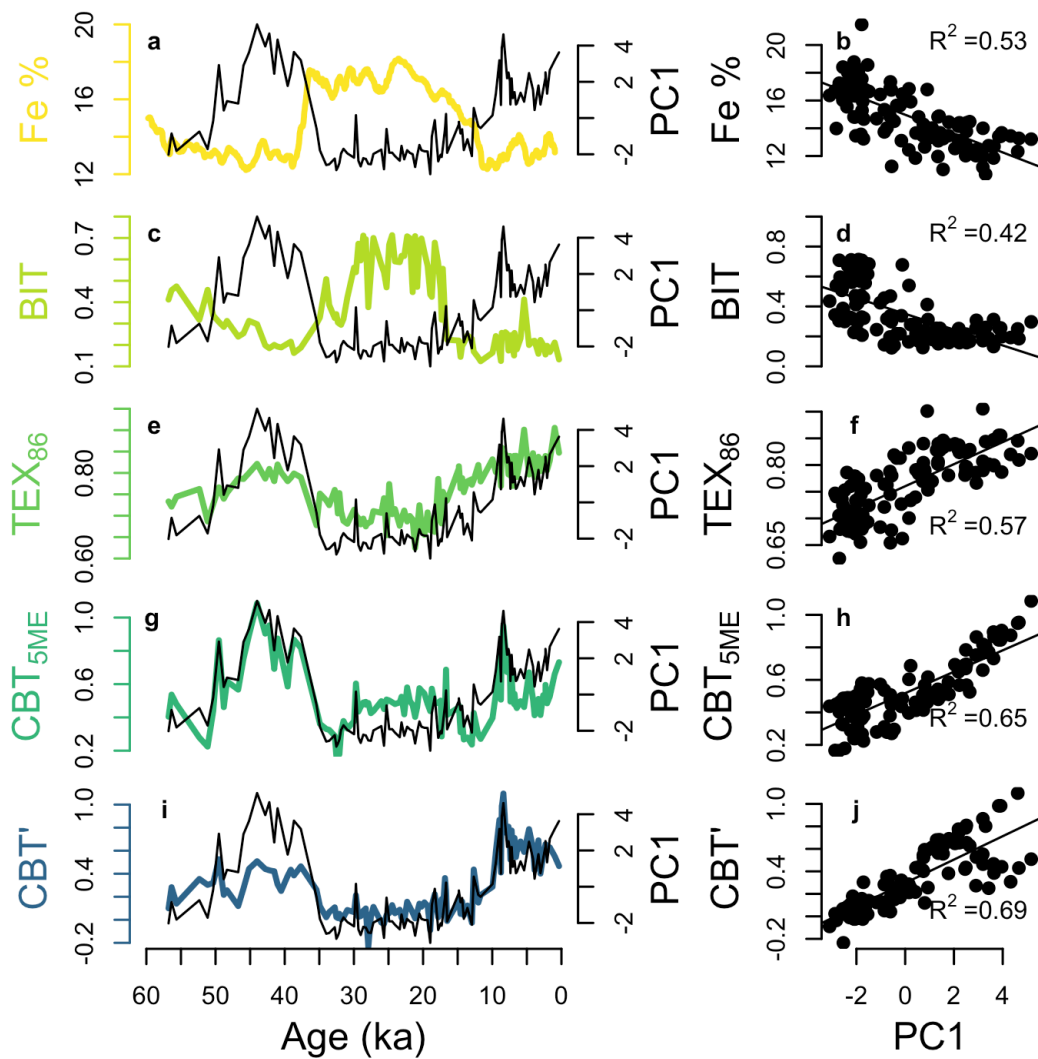


Figure S2. (a) Iron content from the Towuti lake sediment core (Costa et al., 2015). (c) Lake Towuti BIT index. (e) TEX₈₆. (g) The CBT_{5ME} index. (i) The CBT' index. Panels on the right (b, d, f, h, and j) show R² values from linear regressions between the variables on the left and PC1 from the principal component analysis shown in Figure 4 (black).

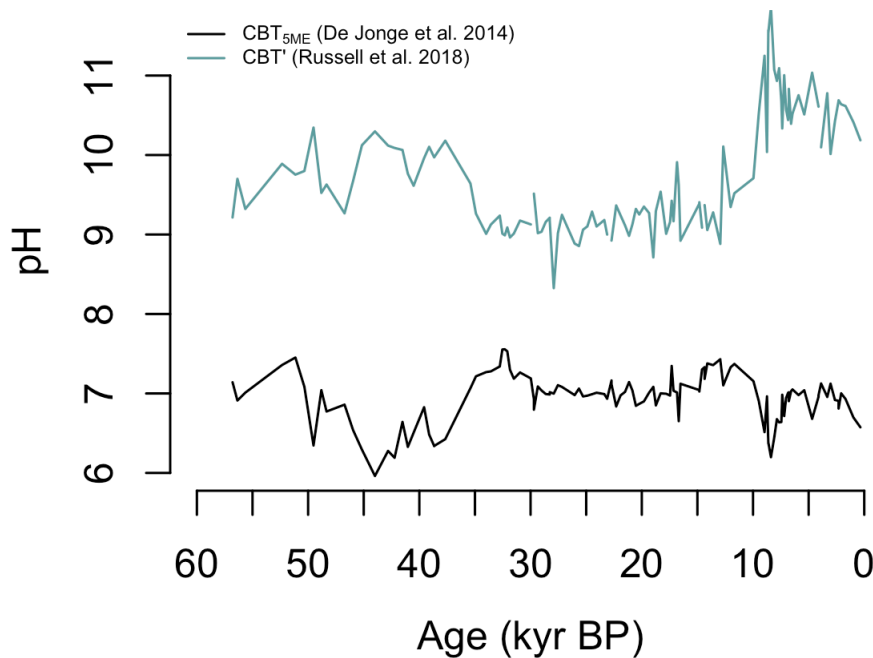


Figure S3. Reconstructions of pH using the CBT_{5ME} -based calibration (black) and the CBT' -based calibration (teal). The equations are shown below. The records show opposite trends because the De Jonge et al. (2014) calibration has a negative slope and the Russell et al. (2018) calibration has a positive slope, which may be caused by a weak sensitivity to pH in tropical East African lakes.

$$CBT_{5ME} = -\log\left(\frac{Ib + IIb}{Ia + IIa}\right) \quad \text{De Jonge et al. (2014)}$$

$$pH = 7.84 - 1.73 \times CBT_{5ME} \quad \text{De Jonge et al. (2014)}$$

$$CBT' = -\log\left(\frac{Ic + IIa' + IIb' + IIc' + IIIa' + IIIb' + IIIc'}{Ia + IIa + IIIa}\right) \quad \text{De Jonge et al. (2014)}$$

$$pH = 8.95 + 2.65 \times CBT' \quad \text{Russell et al. (2018)}$$